CHALMERS
UNIVERSITY OF TECHNOLOGY

Feasibility study of GOCoated WCCo-Cr porous powder for improved wear resistance in HVAF coatings

Surfaces and Interfaces 86 (2026) 108721

Contents lists available at ScienceDirect

Surfaces and Interfaces

journal homepage: www.sciencedirect.com/journal/surfaces-and-interfaces

Feasibility study of GO—Coated WC—Co-Cr porous powder for improved wear resistance in HVAF coatings

Plinio Fernandes [a,*], Jinhua Sun [a], Eric Tam [a], Stefan Björklund [b], Antonin Riche [b], Shrikant Joshi [b], Uta Klement [a]

[a] Department of Industrial and Materials Science, Chalmers University of Technology, Gothenburg, Sweden
[b] Department of Engineering Science, University West, Trollhättan, Sweden

ARTICLE INFO

Keywords:
GO incorporation
Molecular-level mixing
Thermal spray coatings
HVAF
Wear resistance

ABSTRACT

Wear-induced failures in mechanical components remain a critical challenge in industrial applications, necessitating advanced surface engineering solutions. Thermal spraying, particularly high-velocity air fuel (HVAF), is a potential technique for depositing wear-resistant coatings. WC—Co-Cr is extensively used due to its exceptional hardness, ductility, and corrosion resistance. Recent studies have explored the incorporation of carbon nanomaterials to enhance the tribological performance of WC—Co-Cr coatings, with promising results. Among these, graphene oxide (GO) offers distinct advantages, including cost-effectiveness, processing versatility and layered structure, making it a suitable candidate for wear-resistant coatings. However, achieving uniform distribution and strong interfacial bonding within the matrix remains a challenge. This work presents a feasibility study of a novel approach for incorporating GO into HVAF sprayed WC—Co-Cr coatings using a non-commercial porous powder. GO was bonded to the powder surface through a molecular-level mixing process, allowing partial coverage of both the outer surface and inside the pores. The GO-coated powders and the resulting HVAF coatings were characterized using SEM, Raman spectroscopy, TGA, and XPS. GO was found throughout the HVAF coatings, illustrating the advantages of the molecular-level mixing process and the use of porous powder to protect the GO in the spraying process. Tribological tests showed that the GO-reinforced coatings exhibited 10.5% higher hardness, reduced the average friction coefficient in the as-sprayed state from 0.68 to 0.58, and reduced porosity from 13% to 9% compared to coatings with the virgin porous WC—Co-Cr powder. The results show that GO can be successfully incorporated into HVAF coatings, leading to improved lubrication and wear resistance compared with the original powder. Nevertheless, prolonged wear testing indicated that GO gradually degrades over time.

1. Introduction

Wear of mechanical parts in sliding contact is still a major cause of failures and accidents. As these issues predominantly occur at the surface, mitigation strategies have been explored, including surface treatments, coatings, and lubricants [1,2]. Coatings are a promising solution as they provide a wear resistant layer while maintaining the required mechanical properties of the bulk material. Thermal spraying is a widely accepted manufacturing process for applying coatings to protect against erosion, corrosion, and thermal degradation. Within the spectrum of thermal spraying technologies, high velocity oxy fuel (HVOF) and high velocity air fuel (HVAF) are particularly effective for the deposition of metallic coatings [3]. In addition to differences in fuel composition, HVAF operates at lower temperature and higher speed, being more suitable for materials sensitive to thermal degradation [4].

WC—Co-Cr is a widely used material for wear resistance coatings due to its high hardness and good corrosion resistance [5–7]. The tungsten carbide (WC) grains provide exceptional hardness, while the cobalt-chromium binder provides ductility and toughness, which its chromium content offers improved corrosion resistance compared with pure Co binders [8,9]. Further improvements in erosion and corrosion resistance for WC—Co-Cr coatings were investigated by adding different materials as feedstock powders through powder blending [10], nanoscale powders [4], and intermediate layers [11]. These thermal spray coatings are widely used in extreme conditions, offering high wear resistance and surface protection in industries such as metallurgy, mining, and oil extraction [12].

Recent studies have demonstrated the potential of carbon

* Correspondence author.
E-mail address: plinio@chalmers.se (P. Fernandes).

https://doi.org/10.1016/j.surfin.2026.108721
Received 19 June 2025; Received in revised form 29 January 2026; Accepted 9 February 2026
Available online 11 February 2026

nanomaterials to improve the tribological properties of WC—Co-Cr coatings [13]. For instance, Venturi et al. [12] successfully incorporated carbon nanotubes (CNT) into a WC—Co thermal spray coating by spraying an aqueous suspension containing CNTs, commercial WC—Co powder, and a surfactant to mitigate CNT agglomeration. The authors employed an internal diameter high-velocity oxy-air fuel (ID-HVOAF) process, a modified thermal spraying technique designed for coating inner surfaces of narrow tubes, cylinders, and pipes. In this configuration, modifications such as a reduced combustion chamber, smaller and reoriented nozzle, and adjusted oxygen/air flow rates lower the flame temperature and shorten particle residence time, which helps mitigate CNT degradation during spraying. The resulting coatings exhibited low porosity (up to 4 %) along with improvements in coefficient of friction, microhardness, and wear rate. The authors concluded that variations in spray parameters and CNT concentration are critical in determining the final properties of the thermally sprayed coating; they can reduce porosity and improve performance at optimal levels, but excessive CNT content can decrease fracture toughness and lead to instability during wear testing. Similarly, Kumar and Verma [14] mixed commercially available WC—Co-Cr and graphene nanoplatelets (GNP) in concentrations ranging from 1 to 4 wt % and deposited the material by standard high-velocity oxygen fuel (HVOF) spraying. Their results showed improvements at room temperature including a reduction in porosity from 3.8 % to 1.5 %, a decrease in coefficient of friction from 0.26 to 0.16, and a reduction in wear rate from 0.195 to 0.071. These improvements were attributed to GNPs filling coating porosity and acting as solid lubricants. However, the best results were achieved with an addition of 2 wt % GNP, suggesting that excessive GNP levels may be detrimental.

The mechanisms underlying the tribological improvements brought about by graphene and its derivatives were also investigated. Xu et al. [15] investigated the anti-friction mechanisms of various graphene-based materials, including physical vapor deposition monolayer graphene (PMG), nitrogen doped graphene (NG), fluorinated graphene (FG), graphene oxide (GO), and GNP. These materials were dispersed in high-purity ethanol at different concentrations and applied onto 304 stainless steel substrates by drop casting. The authors concluded that the primary lubrication mechanism of all graphene species studied is based on their ability to delaminate and form an adsorbed tribofilm (tribolayer), thereby acting as solid lubricants. However, they also demonstrated that the concentration of the graphene solutions and the specific drop casting conditions play a crucial role in the formation and effectiveness of the tribolayer.

Graphene oxide is another promising carbon nanomaterial for enhancing the tribological properties of thermal spray coatings. In addition, GO is particularly attractive due to its process versatility, layered structure and lower cost in comparison to other forms of graphene [16,17]. GO is produced by chemical exfoliation manufacturing process that allows reliable, cost-effective and large-scale production compared to the more expensive production methods, such as chemical vapor deposition (CVD) [18]. However, challenges arise with distribution and interfacial bonding with the matrix when incorporating GO into metal matrix composites [19]. One strategy to overcome these challenges is the use of a molecular-level mixing process to chemically bond GO onto the metal powder particles, with a coupling agent [20,21]. Due to the abundance of oxygen functional groups on the surface of GO, organic surfactants such as silanes can serve as bridging agents, bonding GO to the metal surface [22]. This method offers a versatile alternative for coating GO onto various metal powders, not sharing limitations associated with shape and electrical conductivity, which are common in techniques like electrophoretic deposition (EPD) [23].

In this study, we investigate a novel approach for incorporating GO into thermal spray coatings produced by HVAF to increase wear resistance. The incorporation method, based on a molecular-level mixing strategy, enables the coating of GO with controllable characteristics on both the outer and inner surfaces of the porous powders, increasing the potential for better dispersibility. A non-commercial porous WC—Co-Cr powder was used as the matrix, which allowed GO to be deposited not only on the powder surface but also the inside pores, where it was additionally protected during the HVAF process. First, the GO coating process was investigated to evaluate the effectiveness of the proposed process in depositing GO on the surface and in the pores of the WC—Co-Cr powder particles. Subsequently, the GO-containing WC—Co-Cr powder was used in the HVAF thermal spray process to produce coatings. A detailed characterization was performed to investigate the morphology and extent of GO coverage on the powder as well as to evaluate the retention of GO in the coatings after the HVAF process. The effect of GO addition on the tribological properties of the thermal spray coatings was investigated. The results demonstrate the feasibility of this innovative strategy for incorporating GO into thermal spray coatings and provide valuable insights into its potential for improving wear resistance.

2. Materials and methods

2.1. Graphene oxide coating process

The synthesis procedure of the GO coated WC—Co-Cr powder (which will be referred to as *GO-containing WC—Co-Cr powder*) was divided into three simple steps: 1) surface functionalization of the WC—Co-Cr particles, 2) GO incorporation, and 3) drying. During the surface functionalization step the WC—Co-Cr powder (which will be referred as *virgin powder*) was dispersed in toluene at a concentration of 200 g/l. The WC—Co-Cr porous powder used was a non-commercial grade 558.444 provided by Höganäs AB, with a powder size ranging from 25 to 55 μm (see Fig S2), and the toluene was analytical grade from Supelco. Then, 3-aminopropyltriethoxysilane (APTES 99 %, Sigma Aldrich) was added to the mixture with a concentration of 0.5 vol %. This mixture was stirred vigorously in a closed glass bottle using a magnetic stirrer for 24 h. After functionalization, the excess solvent was discarded, and the remaining wet powder was rinsed three times with toluene to remove unreacted APTES and washed another three times with deionized water.

The GO incorporation stage started by dispersing GO in 500 ml of water to achieve a concentration of 0.2 g/l. The GO used was obtained from LayerOne and was a de-acidified aqueous paste with 10 wt % concentration, 3– 5 number of layers (as measured by Raman), 3.1 C/O atomic ratio (as measured by X-ray photoelectron spectroscopy), and with a freeze-dried GO lateral size of 2– 20 μm. The pH of this diluted solution was then measured and adjusted to 7 using 0.5 to 1 ml of 1 M ammonium hydroxide solution. In parallel, the APTES functionalized WC—Co-Cr powder was stirred with 500 ml of deionized water. After 1 hour of stirring, the diluted GO solution was added to the functionalized virgin powder and stirred for another 5 min .

In the drying step, the excess water was removed. Dried GO-containing WC—Co-Cr powder was obtained after drying in an oven at 40 °C for 12 h.

2.2. Thermal spraying of GO-containing WC—Co-Cr powder

The HVAF thermal spray process was conducted using the M3 HVAF gun (Uniquecoat Technologies LLC, Oilville, USA) to deposit both virgin powder and GO-containing WC—Co-Cr powder onto Domex steel substrates. The detailed spray deposition parameters are summarized in Table 1. The thermal spray coating using the virgin powder will be referred to as virgin sample, while the coating produced from the GO-containing WC—Co-Cr powder will be called GO-containing WC—Co-Cr sample.

2.3. Mechanical properties of the thermal sprayed coatings

Optical microscopy (OM) was used to determine the thickness and porosity of the thermal spray coatings. Images of cross-sections of both virgin sample and GO-containing WC—Co-Cr were captured using a

Table 1
Parameters used for the HVAF spraying.

Parameters	
Nozzle	5L4
Chamber	M3/3
Injector	#3
Air pressure PSI	113
Fuel 1 pressure PSI	105
Fuel 2 pressure PSI	115
Carrier gas l/min	60
Feeder (V1, V4, G4)	G4
Feed g/min	200
SoD standoff mm	300
Surface speed m/min	115
Step mm/rev	5

Zeiss AxioVision 7 microscope equipped with a Zeiss digital camera 35 and AxioVision software. Porosity was obtained by image analysis using the contrast threshold method [24] applied to 25 images, while thickness was determined by averaging over 50 measurements.

Vickers hardness measurements were performed on polished cross-sectional samples to determine the influence of GO addition on the HVAF sprayed WC—Co-Cr coatings. The equipment used was a Struers Durascan 70G5 (Ballerup, Denmark) with an applied load of 500 g, and for each test 10 indentations were made, and the average value determined.

2.4. Wear testing of GO-containing WC—Co-Cr sprayed coatings

The influence of GO addition on the coefficient of friction (CoF) and specific wear rate (SWR) was investigated by ball-on-disc (BoD) sliding tests. A TRB3 ball-on-disc tribometer from Anton Paar was used. Tests were carried out on different types of thermal spray samples: as-sprayed samples, polished samples, and samples where the top ~50 μm of the surface were ground off. The parameters employed during BoD testing are summarized in Table 2. The grinding was done with a PowerPro 5000 (Buehler) variable speed grinder-polisher. An alumina ball was selected to minimize chemical interactions during wear testing, while a 20 N load was applied to simulate aggressive wear conditions. The surface roughness of the as-sprayed samples was analyzed using a Surftest 301 Mitutoyo equipment.

2.5. Characterization of the GO-containing WC—Co-Cr powder

A FEGSEM LEO-1550 Zeiss Gemini scanning electron microscopy (SEM) was used to examine the morphology of the WC powder and to visualize the GO coating on the coated powder. An acceleration voltage of 5 kV was used, and images were captured for both the virgin powder and the GO-containing WC—Co-Cr powder samples. A WITec alpha 300R Raman microscope was used for both point analysis and Raman mapping. For the mapping, an integration time of 0.05 s was used. Moreover, a summation filter was applied to the data to select the signal around the G peak (1580 cm^{-1}) with a width range of ± 75 cm^{-1}. SEM imaging and Raman spectroscopy were performed on the powder surface, powder cross-section, as-spray HVAF coatings, and coatings after wear testing. Epoxy resin mounting and polishing were used to obtain cross-sectional powder samples. TGA measurements were performed in a Mettler Toledo TGA/DSC3+ instrument using standard Al2O3 crucibles. The primary objective of the TGA analysis was to evaluate the thermal stability of the GO coating when exposed to elevated temperatures. The temperature range was 25 to 900 °C, at four different heating rates (HRs),10, 50, 100, and 150 °C/min . All measurements were conducted in air. The powder size distribution of the virgin WC—Co-Cr powder was obtained using a Microtrac Sync laser diffraction powder characterization equipment.

Table 2
Parameters used for BoD tests.

Normal load (N)	Sliding distance (m)	Linear speed (m/s)	Radius (mm)	Ball
20	5000	0.2	9	Alumina

2.6. Characterization of the wear track

Assuming that the wear profile resulting from the BoD test is uniform over the entire wear track, the volume loss could be determined using a white light interferometer (WLI) (Profilim 3D from Filmetrics) by measuring at four different locations along the circular wear track. First, the average cross-sectional area of the track was determined, and the total volume loss was calculated by multiplying the area with the circumference of the wear track. The specific wear rate ($mm^3 \cdot N^{-1} \cdot m^{-1}$) was then defined as V/(P·s), where P is the applied normal load and s is the sliding distance.

2.7. XPS measurements

Surface chemistry of the GO-containing WC—Co-Cr powder, as-sprayed virgin and GO-containing WC—Co-Cr samples, as well as the wear tracks on the polished and ground samples (both virgin and GO-containing WC—Co-Cr samples) were analyzed by X-ray photoelectron spectroscopy (XPS). XPS was used to investigate how the thermal spraying, polishing and grinding processes affect the surface properties of the coating and the retention of GO. The measurements were performed using a PHI5000 VersaProbe III scanning X-ray microprobe equipped with an Al X-ray source (E = 1486.6 eV). Survey scan measurements were carried out in a binding energy range between 0 and 1350 eV with a scanning step size of 1.00 eV to determine the overall composition. With the elements of interest identified, narrow scans were then carried out at individual energy regions with the step size reduced to 0.10 eV. To investigate the detailed characteristics in carbon, the step size in the C1s scan was even reduced to 0.05 eV.

3. Results and discussion

3.1. Graphene oxide coating on WC—Co-Cr powder

Fig. 1 shows the SEM images of the WC—Co-Cr powder before (a) and after (b) adding the GO coating. The porous morphology of the starting powder can be seen in Fig. 1a. During the coating process, not only the top surface of the particles but also the inside of the pores is coated by GO. The contrast difference between the GO-coated areas and the initial virgin powder surface shows that a partial GO coating has been applied. As we demonstrated and systematically studied in the previous work [25], the molecular functionalization of APTES on the surface of the metal particles results in positively charged surface of the WC—Co-Cr, which allows the uniform attachment of the negatively charged GO. The process is controllable to obtain the WC—Co-Cr with different GO coverage. The partial coverage of WC—Co-Cr was employed in this work to preserve uncoated WC—Co-Cr surfaces, thus promoting sufficient inter-splat bonding and mitigating the risk of splat delamination or detachment [26,27]. Fig. 1 (c) and (d) show the GO coating inside a pore and illustrate the successful coating of the inner surface of WC—Co-Cr particles.

The presence of the GO was also confirmed by Raman spectroscopy. Fig. 2 shows the Raman spectrum of GO-containing WC—Co-Cr powder obtained from point analysis, revealing the characteristic GO peaks D, G, 2D, and $D + G$. The I_d/I_g ratio which provides insights into the structural integrity of the GO was measured to be 1.01 for the GO-containing WC—Co-Cr powder. This value is indicative of highly oxidized GO and is beneficial to the GO coating process. The absorption of GO on the APTES functionalized WC—Co-Cr particles occurs predominantly due to the strong electrostatic interactions between the positively charged

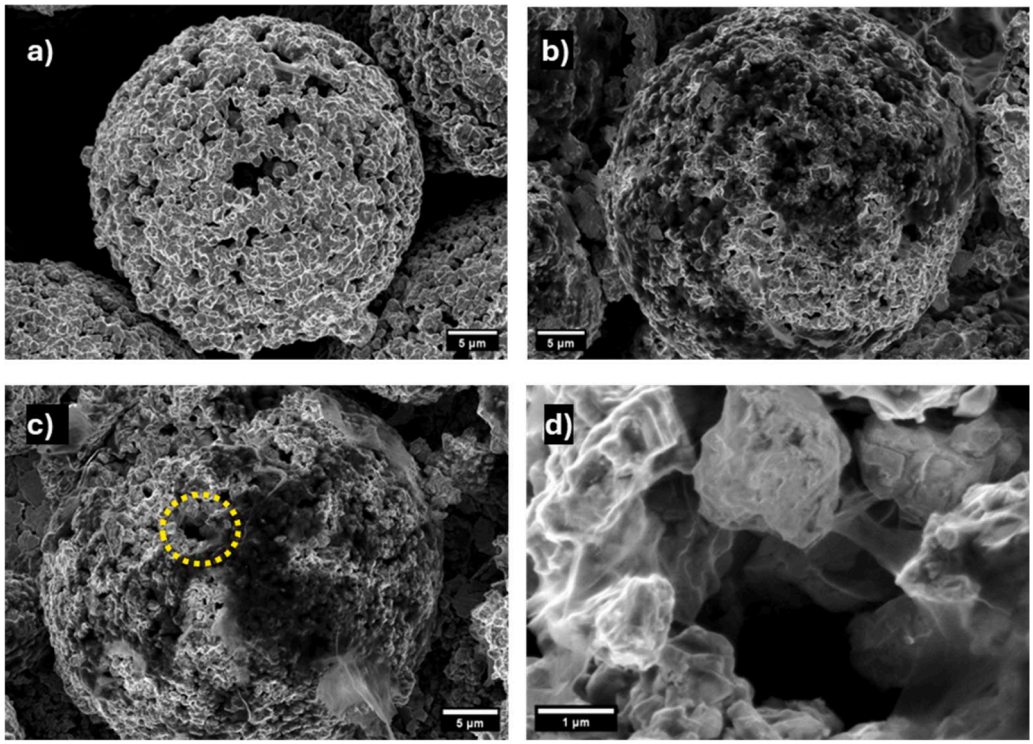

Fig. 1. SEM images of WC—Co-Cr powder before (a) and after (b) application of the GO coating. (c) Powder particle with GO coating visible inside the pores. (d) Magnified inner surface of the pore highlighted in (c).

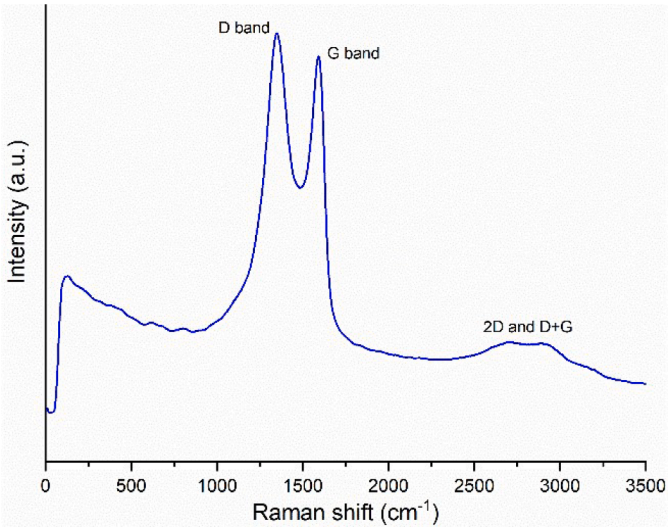

Fig. 2. Raman spectrum of the GO-containing WC—Co-Cr powder.

amine group of APTES and the negatively charged carboxylic functional groups on the GO surface [28,29]. In addition, small traces of tungsten carbide peaks can also be observed as the presence of small Raman peaks between 500 and 900 cm^{-1} [30]. The cross-sectional powder sample was also investigated by Raman mapping to further confirm the presence of GO on the surface and in the pores of particles. Fig. 3 shows the OM image (a) and the respective Raman mapping (b) of a cross-sectioned powder particle. The bright areas in the Raman map (highlighted in green dashed circles) correspond to the regions with a higher intensity of the G peak, clearly indicating the presence of GO in the pores of the WC—Co-Cr particle. The bright rim on the right-hand side of Fig. 3 (b) illustrates that GO is present on the outer surface of the particle (partial coating). Confirmation of GO deposition in the pores increases the probability that this GO fraction is protected from direct impact of the air-fuel jet, increasing its chances of survival during the process. The degradation of graphene derivatives during thermal spraying is a known problem that has already been addressed by different approaches. These include dispersing graphene derivatives in a suspension and adjusting its injection in the spray gun to minimize exposure to the flame [31,32], as well employing lower-temperature deposition techniques such as cold spray [33].

Fig. 4 shows the TGA curves of virgin powder and GO-containing WC—Co-Cr powder across all heating rates measured. The GO incorporation has no significant influence on the thermal stability of the WC—Co-Cr particles at the same heating rate. However, increasing the heating rate caused a shift of the initial oxidation temperature, raising it from approximately 550 °C at 10 °C /min to over 600 °C at 150 °C /min .

This observation suggests that lower heating rates lead to GO degradation due to the prolonged exposure of the incorporated GO to high temperatures. However, at higher heating rates, the GO is exposed to elevated temperatures for a shorter period, increasing its probability of survival. Therefore, manufacturing processes with high heating rates such as HVAF are advantageous for maintaining the deposited GO on the powder. It is also relevant to mention that the HVAF process is characterized by extremely high in-flight velocities of the injected powder particles leading to their extremely short residence times, typically of the order of ms. This, too, is likely to facilitate GO retention during spraying.

3.2. *Thermal spraying of GO-containing WC—Co-Cr*

Fig. 5 shows the SEM images of the virgin sample (a) and GO-containing WC—Co-Cr sample (b). Both coatings exhibit a rough and porous morphology across the entire sample, with no influence of the GO incorporation on the surface roughness of the thermal sprayed coating, as shown in Fig. S3. In the GO-containing WC—Co-Cr sample, the GO is observed as thin, layered structures with a darker contrast relative to the lighter WC—Co-Cr matrix. At high magnification (Fig. 5

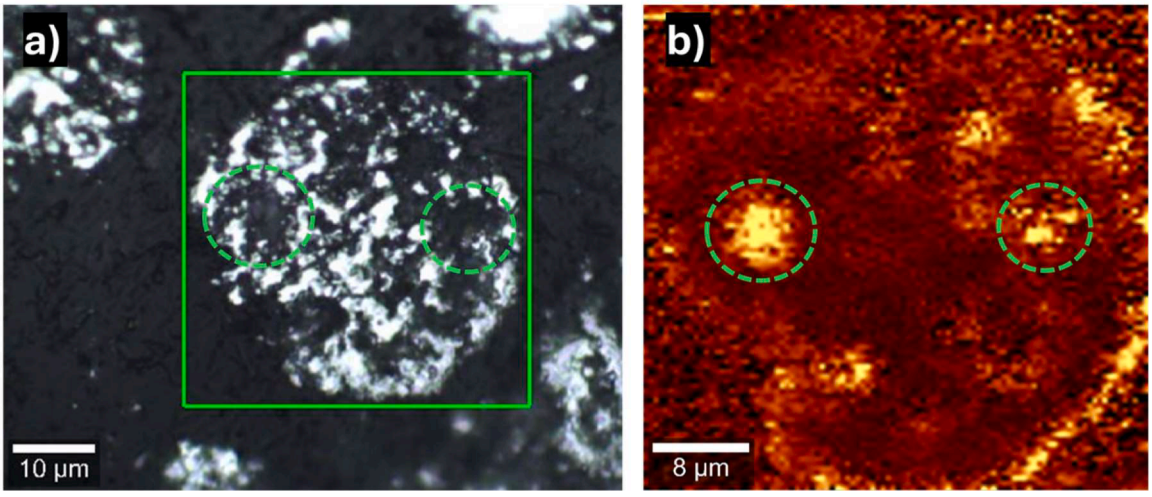

Fig. 3. a) OM image of a cross-sectioned GO-containing WC—Co-Cr powder particle; b) Raman map of the respective particle.

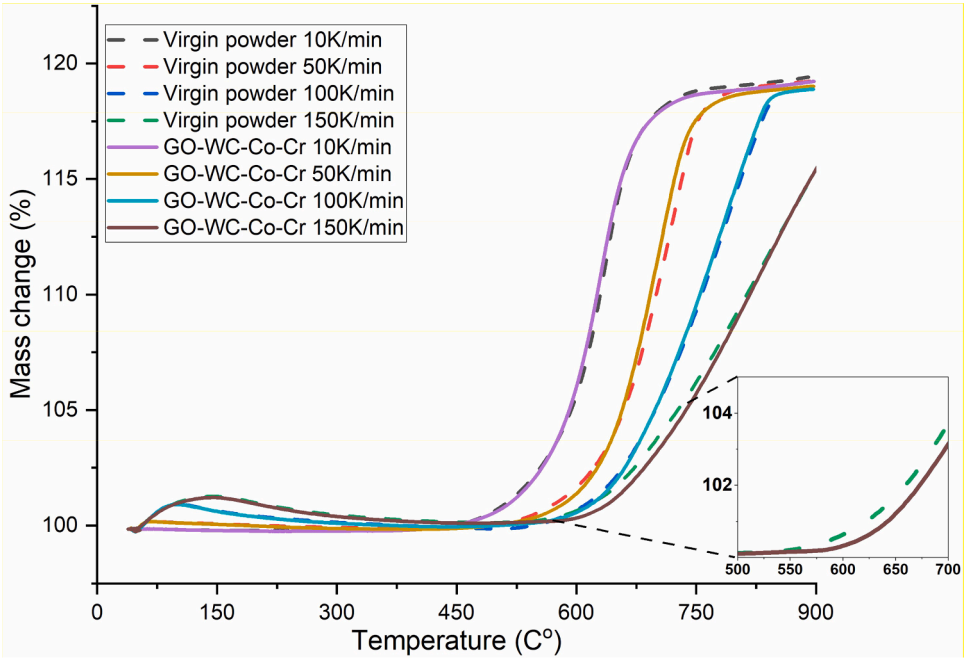

Fig. 4. Mass change of virgin powder and GO-containing WC—Co-Cr powder (GO-WC—Co-Cr) in the image) across all heating rates. The inset shows the oxidation temperature shift for the 150 °C/min sample.

(b) and (c)), the presence of the GO can be confirmed by its characteristic wrinkled morphology. The GO flakes distributed throughout the WC—Co-Cr matrix are on the order of a few micrometers in size, and their morphology remains distinguishable after the HVAF process, which can be seen by comparing with Fig. 1 (b) and (d). In the polished cross-section sample in Fig. 6 (d), GO flakes are shown inside a pore and adhered to its inner surface. These observations confirm the success of the GO incorporation method in combination with the porous morphology of the powder, in both the retention of GO after the HVAF process and mitigation of GO agglomeration.

The presence of GO after HVAF spraying was further confirmed by Raman spectroscopy. Fig. 6 shows the OM image (a) alongside the corresponding Raman mapping (b) of the highlighted area. The Raman map reveals bright spots, indicating regions with a higher concentration of GO. A comparative Raman map of the as sprayed WC—Co-Cr can be found in the supplementary image S3.

Raman mapping was also employed to examine the presence of GO on the cross-section of the thermal sprayed coating. Fig. 6 exhibits the OM image (Fig. 6 c) and the Raman mapping (Fig. 6 d) of the polished cross-sectional sample. It is worth noting that the dark spots observed in Fig. 6 (c) are pores, which may or may not contain GO on their inner surface. Therefore, these features should not be misinterpreted as GO, as the thin layered morphology of GO is not detectable with the resolution of an optical microscope.

Table 3 provides measurements of porosity, thickness, and hardness of the thermal spray samples. The measurements were performed on polished cross-sections of both the virgin and GO-containing WC—Co-Cr samples.

The porosity values found in both virgin and GO-containing WC—Co-Cr samples are significantly higher than the state-of-the-art density values achieved with commercial WC—Co-Cr powders, which have a well-established process window that enables the production of nearly fully dense coatings with excellent mechanical properties, such as hardness and toughness [34]. Torkashvand et al. [35] conducted a

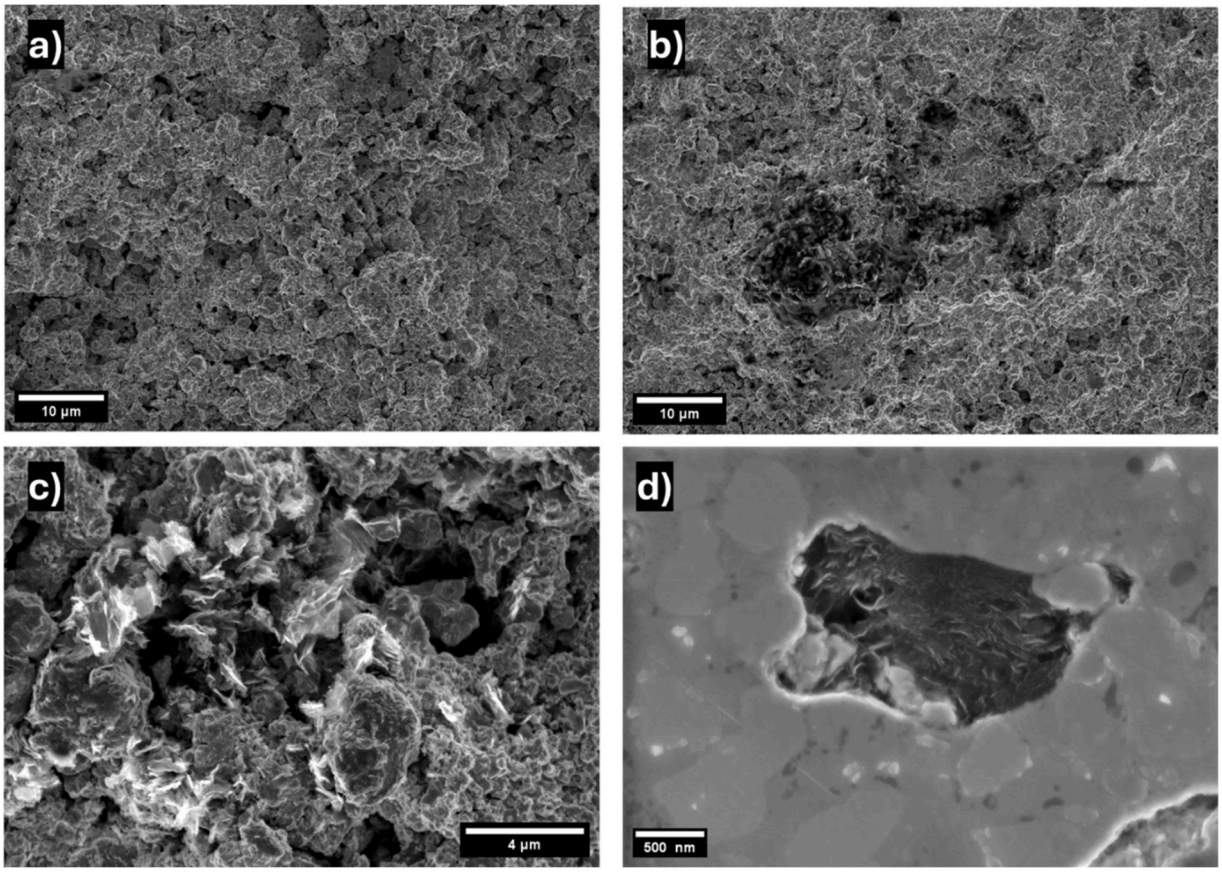

Fig. 5. SEM images of the HVAF sprayed samples. a) Top-view of WC. b) Top-view of GO-containing WC—Co-Cr sample. c) GO flakes in the sprayed GO-containing WC—Co-Cr sample. d) GO flakes adhered to the inner surface of the pore in the cross-sectional polished GO-containing WC—Co-Cr sample.

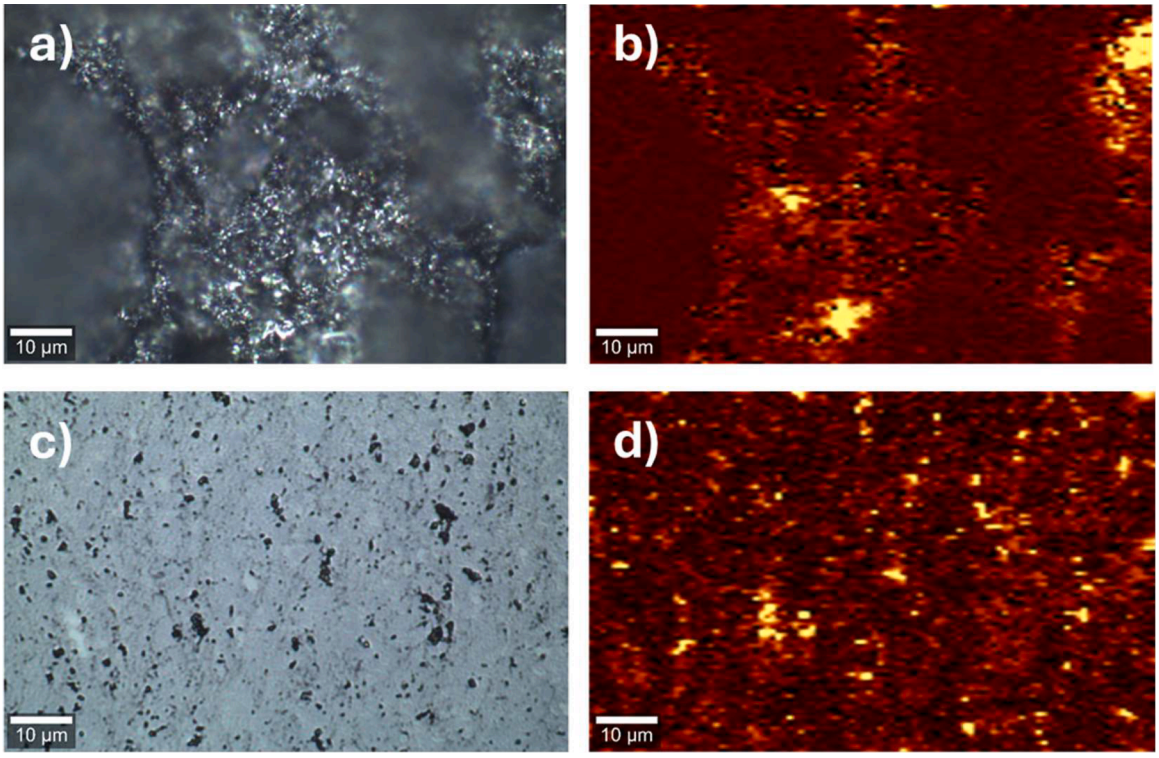

Fig. 6. OM images (a, c) and Raman maps (b, d) of GO-containing WC—Co-Cr samples in as-sprayed condition (a, b) and cross-sectioned and polished (c, d).

Table 3
Results of microstructural and mechanical analysis of the HVAF sprayed coatings.

	Virgin sample	GO-containing WC—Co-Cr sample
Porosity (%)	13.22 (±0.83)	9.08 (±0.61)
Thickness (μm)	147.19 (±8.48)	125.70 (±6.77)
Hardness (HV)	1086.9 (±90.97)	1213.3 (±73.38)

benchmark study evaluating different nozzle configurations and particle sizes of commercial WC—Co-Cr powder to optimize coating performance for wear resistance. Their results showed very low porosity and high hardness, reaching up to HV 1600. They concluded that, for a fixed nozzle configuration, reducing the powder size decreased porosity, enhanced hardness, and improved wear resistance. Kumar and Verma [14], also using a commercial WC—Co-Cr powder, reported an initial porosity of 3.83 %, which was further reduced to 1.55 % with the incorporation of 4 wt % GNPs, demonstrating that GNP addition can also promote low-porosity WC—Co-Cr thermal-sprayed coatings.

In contrast, the WC—Co-Cr powder used in this study was a non-commercial porous grade, deliberately selected to enable the protection of GO within its pores, as previously discussed. Consequently, the relatively high porosity observed in both virgin and GO-containing WC—Co-Cr samples deviates from the benchmark values reported in the literature and can be primarily attributed to the inherent porosity of the starting powder. Nevertheless, the GO-containing WC—Co-Cr sample has a significantly lower porosity, about 4 % reduction as compare with the virgin sample, as seen in Table 3 and Fig. 7. For composites, a reduction in porosity is commonly justified by a filler effect where reinforcements occupy voids in the matrix, thereby decreasing overall porosity [32]. This mechanism was also identified by Kumar and Verma [14] to explain the porosity reduction in their GNP reinforced thermal spraying coatings. However, given the small GO content, this cannot be the only reason. The reduction of the porosity is due to the improvement of the thermal conductivity of the GO-containing WC—Co-Cr powder, which facilitates a more uniform temperature distribution during the HVAF process, promoting densification and reducing porosity of the sprayed coating [12,27]. The concept of a critical bonding temperature has been discussed in thermal spraying of ceramics, where each sprayed material system has a specific temperature in the interface between the impacting molten particles and the splats that must be exceeded for bonding to occur. In regions where the interface temperature remains below this critical value, porosity can emerge [27]. Consequently, the presence of GO on the virgin powder acts as a preferential heat path, thus enabling a more uniform heat distribution and increasing the probability of overcoming the critical bonding temperature across more interface regions, reducing porosity [36].

The mechanical integrity of the thermal spray coating was evaluated by Vickers hardness testing on the cross-sectional samples. It is well-known that wear resistance is proportional to the hardness of the material, which is a key reason for WC being widely used as wear-protection coating [37]. The 10 % increase in hardness as shown in Table 3 is due to the addition of GO to the virgin powder as it increased the density of the thermal spray coating. Porosity acts as voids during hardness measurements such as the Vickers test, where pores beneath the indenter reduce the effective contact area and limit the amount of solid material available to sustain the applied load. Moreover, pores serve as stress concentrators, increasing the likelihood of crack initiation under indentation and thereby contributing to lower measured hardness values. Despite the relatively high porosity of both coatings, the hardness values obtained in this study fall within the range of 900–1300 HV reported in the literature for GNP reinforced WC—Co-Cr thermal-sprayed coatings [13], demonstrating that the GO-containing coating exhibits hardness values comparable to those expected for similar WC—Co-Cr systems.

3.3. Wear tests on thermal sprayed coatings

Fig. 8 (a) shows the evolution of the coefficient of friction (CoF) of both the GO-containing WC—Co-Cr sample and the virgin sample. While the curves for the two thermal spray samples show similar trends, the presence of incorporated GO in WC—Co-Cr (GO-containing WC—Co-Cr sample) results in a lower CoF, as observed from the average measured values of CoF for the two types of coating. The virgin sample exhibits an average CoF of 0.68 (± 0.03) whereas the addition of GO in the GO-containing WC—Co-Cr sample lowers the average CoF to 0.58 (± 0.02). This result confirms that the addition of GO could improve the lubricity of the WC—Co-Cr sprayed coating. In the as-spray condition, the lubricating effect of GO persisted throughout the entire BoD test, most likely because the incorporated GO maintained its layered structure. Under this condition, GO could delaminate effectively during sliding and sustain its lubricating performance for the full duration of the test.

When grinding off about 50 μm of the GO-containing WC—Co-Cr sample, a decrease in CoF is also observed compared to the virgin sample, as shown in Fig. 8 (b). This is due to the presence of GO inside the WC—Co-Cr matrix. However, the curve shape of the ground samples is notably different from the ones observed in Fig. 8 (a). For the ground virgin sample, the CoF had a maximum of 0.8 after about 2000 s before

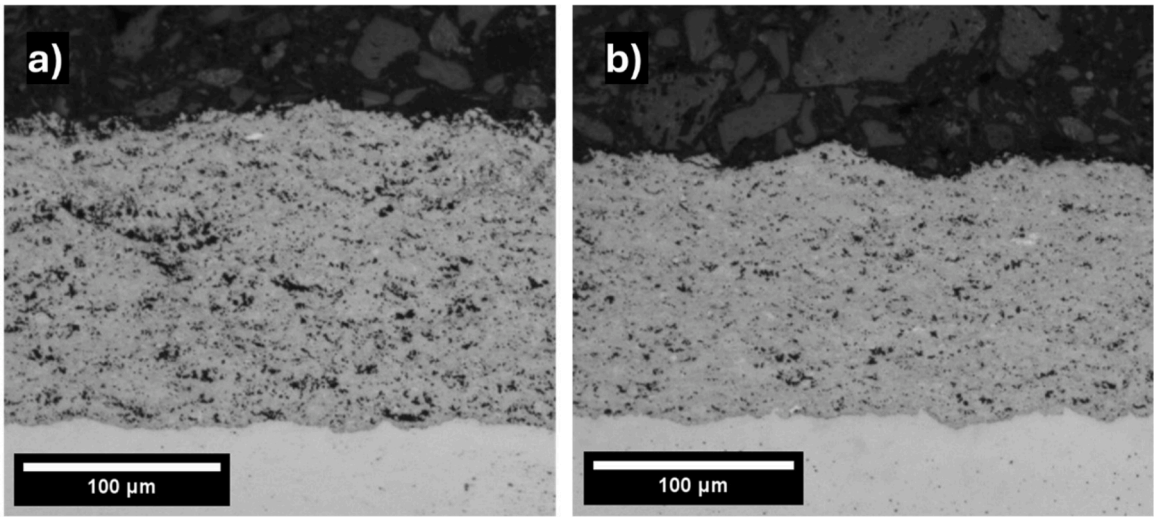

Fig. 7. OM images of the polished cross-section samples of the thermal spray coatings, a) virgin sample (WC—Co-Cr), b) GO-containing WC—Co-Cr sample.

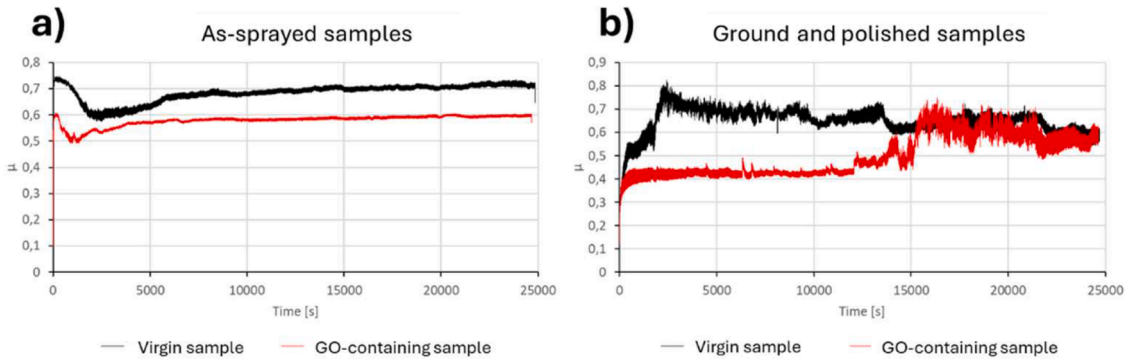

Fig. 8. COF during the BoD wear test for both virgin sample and GO-containing WC—Co-Cr sample (GO-containing sample). a) As-sprayed samples. b) Ground and polished sample.

subsequently decreasing to a value of 0.6. On the other hand, the GO-containing WC—Co-Cr sample exhibits a steady state CoF value of about 0.4 up to 12,000 s and then increases to 0.6. The initially low value is an indication that the lubricating effect of GO persists deeper in the coating thickness. However, the subsequent increase in CoF suggests that the BoD test may have compromised the GO and reduced its effectiveness during prolonged wear as reported in previous investigation [38].

It is important to note that the present thermally sprayed coating exhibited higher porosity compared with the low-porosity benchmark coatings reported in the literature. This difference likely explains the relatively higher CoF values measured in this work compared with reported values as low as 0.2 [35,39]. Furthermore, studies involving carbon nanomaterial incorporation also highlight the influence of porosity on friction performance. Venturi et al. [12], for instance, reported large fluctuations in CoF (0.4–0.2) that were attributed to porosity variations. In addition, Kumar and Verma [13] achieved a very low CoF of 0.172 at 4 wt % GNP, yet their 2 wt % sample showed a higher CoF (0.251) than the base coating (0.243), which they also associated with increased porosity. Nevertheless, due to the relatively high porosity of the coatings in the present study, the improvement in CoF resulting from GO incorporation should be evaluated only in comparison with the virgin coating, rather than against benchmark values from literature.

Table 4 shows observed specific wear rates (SWRs) for the ground and polished sample. SWRs are very low in both cases and of the order of 10^{-7} / 10^{-8} mm3/(Nm), which is consistent with previous studies on HVAF sprayed WC coatings [40]. The incorporation of GO slightly lowers the SWR. However, considering the standard deviation, the difference seems insignificant. Similar results were reported by Venturi et al. [12], where the addition of CNTs led to negligible changes in SWR despite an increase in microhardness. The authors attributed this behavior to the fact that even though CNT incorporation improved hardness, it did not enhance fracture toughness, resulting in comparable wear rates for both the virgin and CNT reinforced coatings.

3.4. XPS analysis

The XPS measurements provided detailed insights into the surface chemistry and further evidence of GO incorporation into the thermal sprayed coating. The measurements showed changes in the chemical state of carbon caused by processes such as thermal spraying, polishing, and grinding. These changes in chemical state contributed to understanding the effect of incorporated GO in different wear environments and provided additional support to the observed performance. Fig. 9 shows the C 1 s elemental scan of the virgin sample (a) and GO-containing WC—Co-Cr sample (b) in as-sprayed condition. The GO-containing WC—Co-Cr sample exhibited additional chemical states, including the π-π* state, which indicates the presence of graphene and its derivatives [41].

Fig. 10 presents the C 1 s spectrum of the GO-containing WC—Co-Cr sample under various conditions to evaluate and monitor the behavior of incorporated GO in wear environments. XPS analysis was conducted on the powder and in the wear tracks of the as-spray, polished, and ground samples after the BoD test. The spectra revealed an evolution in binding energies indicative of carbon oxidation, with an increase in oxidized carbon peak intensities and the appearance of new oxidized states, such as COO^- and CO_3^{2-}. Table 5 summarizes the concentrations of the detected chemical states for all samples.

The high concentration of oxidized carbon in the powder was likely due to the oxidized nature of GO. During the thermal spraying process, the oxygen-containing functional groups of GO were thermally reduced, which was reflected in a decrease in the sp^3 state and oxidized states such as C—O and $C = O$. In addition, the appearance of other metal carbides suggests that HVAF processing had some influence on surface chemistry. Polishing introduces both thermal and mechanical stresses, which led to increased surface oxidation and the likely decomposition of GO, with functional groups changing to other chemical states. This step also enhanced the WC state due to the removal of the CoCr metallic binder, as observed in the survey scan. This results in the WC particles becoming more dominant in the wear resistance. In ground and polished samples, the combination of wear testing with abrasive actions (from sandpaper and diamond solutions) further damaged the coating surface. This abrasive force impacts the GO, as reflected in a reduction of the sp^2 bonds and an increase in sp^3 bonds, while the π–π* bonds also show an increase (as seen in Table 5 A and B), suggesting partial GO retention despite significant damage. This observation supports the initial reduction in the coefficient of friction (CoF) during the BoD test for ground/polished samples.

However, at the end of the wear test, the samples exhibit severe surface oxidation, with a higher proportion of oxidized states compared to reduced states, a distinct difference from all other samples analyzed, as shown in Table 5-C. This substantial oxidation aligns with the mechanical and thermal stresses imposed by the combined polishing, grinding, and wear testing processes. These findings strongly support the conclusion that the deterioration of the incorporated GO is responsible for the loss of its lubricating function.

Table 4
Results of specific wear rates of ground WC—Co-Cr samples.

	Virgin sample	GO-containing WC—Co-Cr sample
Specific wear rates [10^{-8} mm^3/(Nm)]	14.65 (±3.00)	11.58 (±2.27)

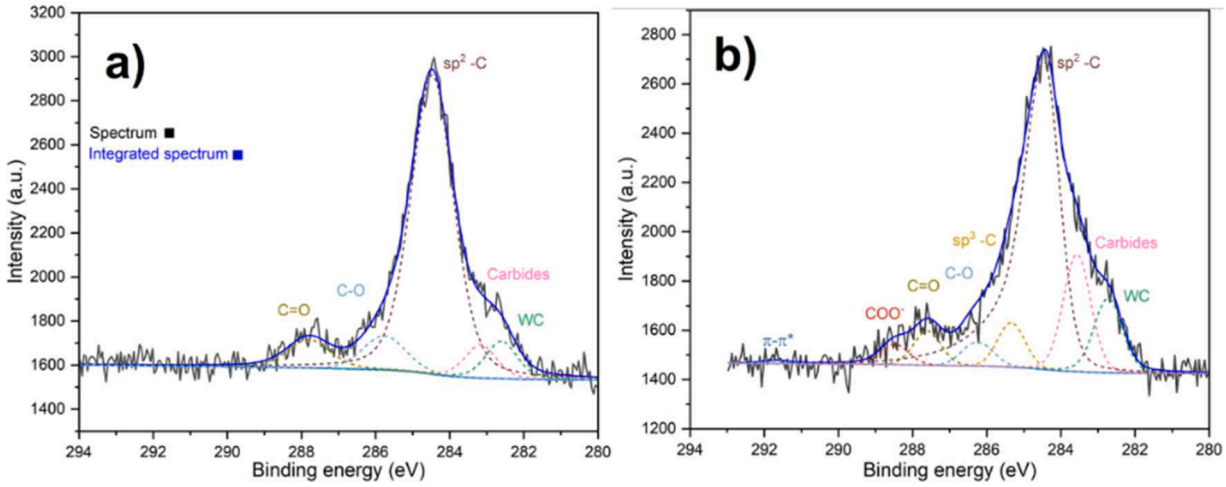

Fig. 9. XPS measurements of the as-sprayed samples at the C1s binding energies. a) Virgin sample. b) GO-containing WC—Co-Cr sample.

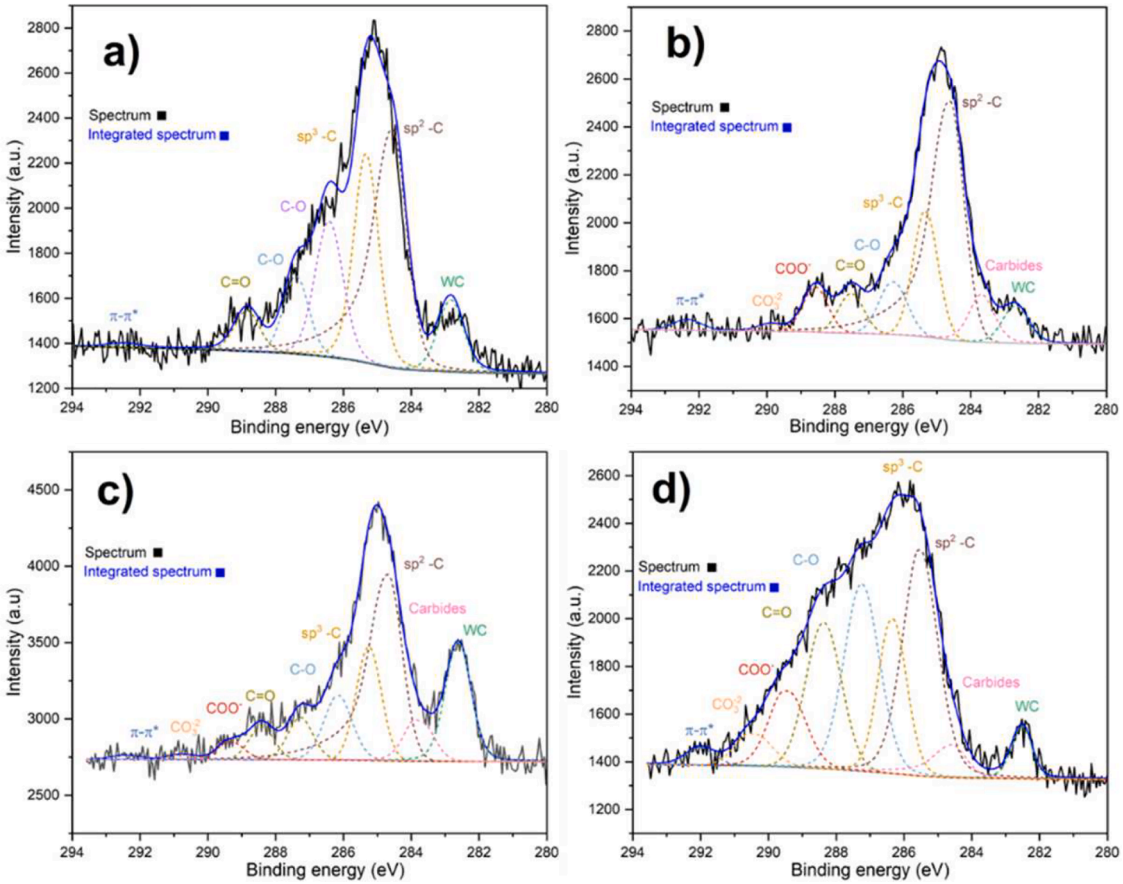

Fig. 10. XPS measurements of GO-containing WC—Co-Cr sample in different conditions. a) Powder. b) Wear track of as-sprayed sample. c) Wear track of polished sample. d) Wear track of ground and polished sample.

4. Conclusion

A GO-coated porous WC-Co-Cr powder was prepared for use in thermal spraying using a molecular-level mixing process. After detailed analysis of the powder and the HVAF-sprayed coatings, the following conclusions were drawn:

- The molecular-level mixing process effectively integrated GO into the WC-Co-Cr powder, as confirmed by SEM, Raman spectroscopy, TGA, and XPS analyses. SEM and Raman also confirmed the deposition of GO on inner surfaces of the porous powder particles.
- SEM imaging and Raman mapping highlighted the improved dispersion of GO in the thermal spray coating, indicating its effectiveness as a solid lubricant for applications in wear-resistant environments.
- The incorporation of GO resulted in a slight reduction in CoF of the samples. However, as this study was a feasibility test for the use of the molecular-level mixing method combined with porous powder,

Table 5
Suggested concentration for carbon chemical states in all GO-containing WC—Co-Cr samples.

A	Reduced states				
Chemical states	WC	M-C	sp2-C	sp3-C	π-π*
Binding energy (eV)	282.7	283.6	284.5	285.2	*>291.0*
GO-containing WC—Co-Cr powder	4.25 %		21.00 %	12.00 %	<0.5 %
GO-containing WC—Co-Cr sample (As-sprayed)	3.50 %	5.00 %	21.50 %	2.00 %	<0.1 %
GO-containing WC—Co-Cr sample (Polished)	9.00 %	3.50 %	19.50 %	8.00 %	0.50 %
GO-containing WC—Co-Cr sample (50 μm grounded)	2.00 %		2.00 %	14.50 %	<1.0 %
B	**Oxidized states**				
Chemical states	sp2-C-O	sp3-C-O	*C = O*	COO-	CO32-
Binding energy (eV)	*285.5 – 286.5*	286.5 – 287.5	287.5 – 288.5	289.0 – 290.5	290.5
GO-containing WC-Co-Cr powder	8.50 %	4.25 %	2.00 %		
GO-containing WC-Co-Cr sample (As-sprayed)	1.00 %	1.50 %	1.00 %		
GO-containing WC-Co-Cr sample (Polished)	5.00 %	3.00 %	2.50 %	1.00 %	<0.5 %
GO-containing WC-Co-Cr sample (50 μm grounded)	7.50 %	11.50 %	8.50 %	5.00 %	2.00 %
C	**Summary of chemical states**				
Samples	**Reduced states**		**Oxidized states**		
GO-containing WC-Co-Cr powder	37.25 %		14.75 %		
GO-containing WC-Co-Cr sample (As-sprayed)	32.00 %		3.50 %		
GO-containing WC-Co-Cr sample (Polished)	40.50 %		11.50 %		
GO-containing WC-Co-Cr sample (50 μm grounded)	18.50 %		34.50 %		

the GO content is not optimized. Nonetheless, the beneficial effects of GO were fully exploited in the as-sprayed samples.

- XPS measurements followed the surface chemistry evolution of the GO-containing material from powder to the ground thermal spray coating sample. Initially, the powder showed a high degree of oxidation due to the oxygen functional groups of GO. The HVAF processing resulted in the reduction of the oxidation levels and sp^3 states of the as-sprayed samples. Subsequent polishing and grinding, in combination with BoD test initially reduced the CoF. However, prolonged wear testing caused premature degradation of GO, ultimately compromising its lubricating properties during extended wear conditions.

This study successfully demonstrated the feasibility of incorporating GO into WC-Co-Cr porous powder to enhance the tribological performance of HVAF-sprayed coatings. The molecular-level mixing process effectively deposited GO onto the powder surface and within its porous structure, ensuring improved dispersion and retention after the HVAF process. The addition of GO led to a reduction in porosity, an increase in hardness, and a lower CoF, indicating enhanced wear resistance and lubrication properties. However, after prolonged wear testing a gradual degradation of GO was observed. Although GO incorporation shows promise for enhancing coating wear resistance, further optimization of both the thermal spraying process and GO content is required. Producing a benchmark-quality coating with optimized GO levels would enable a clearer assessment of GO's potential to further reduce the coefficient of friction without compromising coating integrity. This will be the focus of future work.

Funding

The Chalmers Foundation (Gothenburg, Sweden) financially supported this research on graphene-coated powders led by Uta Klement.

Abbreviations

The following abbreviations are used in this manuscript:
HVAF, High velocity air fuel thermal spray
HVOF, High velocity oxygen fuel thermal spray
HVOAF, High velocity oxy-air fuel
WC, Tungsten carbide
WC-Co-Cr, Tungsten carbide cobalt chromium powder
GO, Graphene oxide
GO-containing, WC-Co-Cr, Graphene oxide coated tungsten carbide-cobalt-chromium Powder
GNP, Graphene nanoplatelets
APTES, 3-aminopropyltriethoxysilane
CVD, Chemical vapor deposition
EDP, Electrophoretic deposition
SEM, Scanning electron microscopy
TGA, Thermogravimetric analysis
XPS, X-ray photoelectron spectroscopy
OM, Optical microscopy
CoF, Coefficient of friction
BoD, Ball-on-disk
SWR, Specific wear rate

During the preparation of this work the author(s) used Grammarly in order to improve the grammar and the coherence of the text. Mendeley reference manager was also used to generate the reference bibliography of this manuscript. After using this tool/service, the author(s) reviewed and edited the content as needed and take(s) full responsibility for the content of the publication.

CRediT authorship contribution statement

Plinio Fernandes: Writing – original draft, Methodology, Investigation, Data curation, Conceptualization. **Jinhua Sun:** Writing – review & editing, Supervision, Conceptualization. **Eric Tam:** Writing – review & editing, Investigation. **Stefan Björklund:** Writing – review & editing, Investigation. **Antonin Riche:** Writing – review & editing, Investigation. **Shrikant Joshi:** Writing – review & editing, Resources, Methodology, Conceptualization. **Uta Klement:** Writing – review & editing, Supervision, Project administration, Methodology, Funding acquisition, Conceptualization.

Declaration of competing interest

The authors declare that they have no known competing financial interests or personal relationships that could have appeared to influence the work reported in this paper.

Supplementary materials

Supplementary material associated with this article can be found, in the online version, at doi:10.1016/j.surfin.2026.108721.

Data availability

Data will be made available on request.

References

[1] P. Gong, Y. Zhang, X. Cui, S. Xu, M. Yang, D. Jia, C. Li, Lubricant transportation mechanism and wear resistance of different arrangement textured turning tools, Tribol. Int. 196 (2024) 109704, https://doi.org/10.1016/j.triboint.2024.109704.

[2] V. Lakkannavar, K.B. Yogesha, C.D. Prasad, R.K. Phanden, G. S., S.C. Prasad, Thermal spray coatings on high-temperature oxidation and corrosion applications – A comprehensive review, Results in Surfaces and Interfaces 16 (2024) 100250, https://doi.org/10.1016/j.rsurfi.2024.100250.

[3] R.K. Guduru, U. Dixit, A. Kumar, A critical review on thermal spray based manufacturing technologies, in: Mater. Today Proc., Elsevier Ltd, 2022, pp. 7265–7269, https://doi.org/10.1016/j.matpr.2022.04.107.

[4] H. Myalska-Głowacka, G. Bolelli, L. Lusvarghi, G. Cios, M. Godzierz, V. Talaniuk, Influence of nano-sized WC addition on the microstructure, residual stress, and tribological properties of WC-Co HVAF-sprayed coatings, Surf. Coat. Technol. 482 (2024) 130696, https://doi.org/10.1016/j.surfcoat.2024.130696.

[5] X. Tan, J. zhang, H. Zhu, Z. Zhang, X. Zhu, W. Ni, T. Li, T. Kuang, H. Dai, X. Zhang, Double layer HVAF-sprayed WC-CoCr coatings for optimal properties, Ceram. Int. 48 (2022) 33992–33998, https://doi.org/10.1016/j.ceramint.2022.07.349.

[6] Q. Wang, S. Zhang, Y. Cheng, J. Xiang, X. Zhao, G. Yang, Wear and corrosion performance of WC-10Co4Cr coatings deposited by different HVOF and HVAF spraying processes, Surf. Coat. Technol. 218 (2013) 127–136, https://doi.org/10.1016/j.surfcoat.2012.12.041.

[7] S.L. Liu, X.P. Zheng, G.Q. Geng, Influence of nano-WC-12Co powder addition in WC-10Co-4Cr AC-HVAF sprayed coatings on wear and erosion behaviour, Wear 269 (2010) 362–367, https://doi.org/10.1016/j.wear.2010.04.019.

[8] S.P. Singh, P.K. Verma, S. Singh, M. Kapoor, R. Balu, Microstructural characterization and electrochemical behaviour of HVOF sprayed WC-Co-Cr coatings on 316L boiler steel stainless steel, Results in Surfaces and Interfaces 16 (2024) 100248, https://doi.org/10.1016/j.rsurfi.2024.100248.

[9] A.R. Govande, A. Chandak, B.R. Sunil, R. Dumpala, Carbide-based thermal spray coatings: A review on performance characteristics and post-treatment, Int. J. Refract. Metals Hard Mater. 103 (2022) 105772, https://doi.org/10.1016/j.ijrmhm.2021.105772.

[10] J. Singh, S. Kumar, S.K. Mohapatra, An erosion and corrosion study on thermally sprayed WC-Co-Cr powder synergized with Mo2C/Y2O3/ZrO2 feedstock powders, Wear 438–439 (2019), https://doi.org/10.1016/j.wear.2019.01.082.

[11] M. Hadad, R. Hitzek, P. Buergler, L. Rohr, S. Siegmann, Wear performance of sandwich structured WC-Co-Cr thermally sprayed coatings using different intermediate layers, Wear 263 (2007) 691–699, https://doi.org/10.1016/j.wear.2006.12.057.

[12] F. Venturi, S. Kamnis, T. Hussain, Internal diameter HVOAF thermal spray of carbon nanotubes reinforced WC-Co composite coatings, Mater. Des. 202 (2021) 109566, https://doi.org/10.1016/j.matdes.2021.109566.

[13] V. Kumar, R. Verma, S. Shrivastava, Microhardness and dry sliding wear behaviour of HVOF sprayed WC-Co-Cr+ graphene nanoplatelets coating, Mater, Today Proc 113 (2023) 106–111, https://doi.org/10.1016/j.matpr.2023.08.044.

[14] V. Kumar, R. Verma, Slurry and sliding wear characterisation of HVOF sprayed WC10Co4Cr+graphene coating on textured marine steel, Tribol. Int. 184 (2023) 108489, https://doi.org/10.1016/j.triboint.2023.108489.

[15] J. Xu, T. Luo, X. Chen, C. Zhang, J. Luo, Nanostructured tribolayer-dependent lubricity of graphene and modified graphene nanoflakes on sliding steel surfaces in humid air, Tribol. Int. 145 (2020) 106203, https://doi.org/10.1016/j.triboint.2020.106203.

[16] N. Kumar, A.T. Kozakov, A.V. Sidashov, A.V. Nicolskii, Tribofilm stability of ionic liquid functionalized graphene-oxide in metallic contact interfaces, J. Mol. Liq. 296 (2019) 111813, https://doi.org/10.1016/j.molliq.2019.111813.

[17] A. Kosari Mehr, D. Pourzadeh, A. Kosari Mehr, F. Farid-Shayegan, A. Lotfi-Kaljahi, A. Mizban, R. Babaei, Development and characterization of corrosion-resistant plasma-sprayed Ni-Al composite coatings via graphene oxide fillers, Ceram. Int. 50 (2024) 55351–55362, https://doi.org/10.1016/j.ceramint.2024.10.393.

[18] B. Vasić, U. Ralević, K. Cvetanović Zobenica, M.M. Smiljanić, R. Gajić, M. Spasenović, S. Vollebregt, Low-friction, wear-resistant, and electrically homogeneous multilayer graphene grown by chemical vapor deposition on molybdenum, Appl. Surf. Sci. 509 (2020) 144792, https://doi.org/10.1016/j.apsusc.2019.144792.

[19] A. Naseer, F. Ahmad, M. Aslam, B.H. Guan, W.S.W. Harun, N. Muhamad, M. R. Raza, R.M. German, A review of processing techniques for graphene-reinforced metal matrix composites, Materials and Manufacturing Processes 34 (2019) 957–985, https://doi.org/10.1080/10426914.2019.1615080.

[20] J. Hwang, T. Yoon, S.H. Jin, J. Lee, T.S. Kim, S.H. Hong, S. Jeon, Enhanced mechanical properties of graphene/copper nanocomposites using a molecular-level mixing process, Advanced Materials 25 (2013) 6724–6729, https://doi.org/10.1002/adma.201302495.

[21] B. Lee, M.Y. Koo, S.H. Jin, K.T. Kim, S.H. Hong, Simultaneous strengthening and toughening of reduced graphene oxide/alumina composites fabricated by molecular-level mixing process, Carbon N. Y. 78 (2014) 212–219, https://doi.org/10.1016/j.carbon.2014.06.074.

[22] R. Bhure, A. Mahapatro, Silicon Based Nanocoatings on Metal Alloys and Their Role in Surface Engineering, Silicon 2 (2010) 117–151, https://doi.org/10.1007/s12633-010-9055-6.

[23] G. Baiocco, D. Salvi, N. Ucciardello, Optimizing Graphene Nanoplatelet Coating for Enhanced Wear Resistance on Copper Through Electrophoretic Deposition Parameters, J. Mater. Eng. Perform. (2024), https://doi.org/10.1007/s11665-024-10544-0.

[24] S.B.A. Malladi, D. Riabov, S. Guo, L. Nyborg, Additive Manufacturing of Interstitial Nitrogen-Strengthened CoCrNi Medium Entropy Alloy, Adv. Eng. Mater. (2024), https://doi.org/10.1002/adem.202401182.

[25] J. Sun, K.H. Martinsen, U. Klement, A. Kovtun, Z. Xia, P.F.B. Silva, E. Hryha, L. Nyborg, V. Palermo, Controllable Coating Graphene Oxide and Silanes on Cu Particles as Dual Protection for Anticorrosion, ACS Appl. Mater. Interfaces 15 (2023) 38857–38866, https://doi.org/10.1021/acsami.3c08042.

[26] J.H. Ouyang, Y.F. Li, Y.Z. Zhang, Y.M. Wang, Y.J. Wang, High-Temperature Solid Lubricants and Self-Lubricating Composites: A Critical Review, Lubricants 10 (2022), https://doi.org/10.3390/lubricants10080177.

[27] C.J. Li, X.T. Luo, S.W. Yao, G.R. Li, C.X. Li, G.J. Yang, The Bonding Formation during Thermal Spraying of Ceramic Coatings: A Review, Journal of Thermal Spray Technology 31 (2022) 780–817, https://doi.org/10.1007/s11666-022-01379-z.

[28] H. Mahdavi, F. Hosseini, Fabrication of high-performance mixed matrix blend membranes comprising PES and TPU reinforced with APTS functionalized-graphene oxide via VIPS-NIPS technique for aqueous dye treatment and antifouling properties, J. Taiwan Inst. Chem. Eng. 142 (2023) 104609, https://doi.org/10.1016/j.jtice.2022.104609.

[29] L. Sánchez-López, B. Chico, I. Llorente, M.L. Escudero, R.M. Lozano, M.C. García-Alonso, Covalent immobilization of graphene oxide on biomedical grade CoCr alloy by an improved multilayer system assembly via Silane/GO bonding, Mater. Chem. Phys. 287 (2022) 126296, https://doi.org/10.1016/j.matchemphys.2022.126296.

[30] R.F. Garcia-Sanchez, T. Ahmido, D. Casimir, S. Baliga, P. Misra, Thermal effects associated with the raman spectroscopy of WO3 gas-sensor materials, Journal of Physical Chemistry A 117 (2013) 13825–13831, https://doi.org/10.1021/jp408303p.

[31] F. Venturi, T. Hussain, Radial Injection in Suspension High Velocity Oxy-Fuel (S-HVOF) Thermal Spray of Graphene Nanoplatelets for Tribology, Journal of Thermal Spray Technology 29 (2020) 255–269, https://doi.org/10.1007/s11666-019-00957-y.

[32] S. Mahade, A. Mulone, S. Björklund, U. Klement, S. Joshi, Incorporation of graphene nano platelets in suspension plasma sprayed alumina coatings for improved tribological properties, Appl. Surf. Sci. 570 (2021) 151227, https://doi.org/10.1016/j.apsusc.2021.151227.

[33] K. Prasad, R.A. Rahman Rashid, N. Hutasoit, S. Palanisamy, N. Hameed, Fabrication of Metal/Graphene Composites via Cold Spray Process: State-of-the-Art and the Way Forward, C-Journal of Carbon Research 8 (2022), https://doi.org/10.3390/c8040065.

[34] V. Matikainen, S. Rubio Peregrina, N. Ojala, H. Koivuluoto, J. Schubert, P. Vuoristo Houdková, Erosion wear performance of WC-10Co4Cr and Cr3C2-25NiCr coatings sprayed with high-velocity thermal spray processes, Surf. Coat. Technol. 370 (2019) 196–212, https://doi.org/10.1016/j.surfcoat.2019.04.067.

[35] K. Torkashvand, M. Gupta, S. Björklund, F. Marra, L. Baiamonte, S. Joshi, Influence of nozzle configuration and particle size on characteristics and sliding wear behaviour of HVAF-sprayed WC-CoCr coatings, Surf. Coat. Technol. 423 (2021) 127585, https://doi.org/10.1016/j.surfcoat.2021.127585.

[36] K. Chen, W. Xiao, Z. Li, J. Wu, K. Hong, X. Ruan, Effect of graphene and carbon nanotubes on the thermal conductivity of WC-Co cemented carbide, Metals (Basel) 9 (2019), https://doi.org/10.3390/met9030377.

[37] R.J.K. Wood, Tribology of thermal sprayed WC-Co coatings, Int. J. Refract. Metals Hard Mater. 28 (2010) 82–94, https://doi.org/10.1016/j.ijrmhm.2009.07.011.

[38] A. Mulone, P.F.B. Silva, H. Yuan, K. Thånell, A. Hitchcock, U. Klement, Synchrotron X-ray spectromicroscopy analysis of wear tested graphene-containing alumina coatings, Carbon N. Y. 227 (2024) 119245, https://doi.org/10.1016/j.carbon.2024.119245.

[39] B. Song, J.W. Murray, R.G. Wellman, Z. Pala, T. Hussain, Dry sliding wear behaviour of HVOF thermal sprayed WC-Co-Cr and WC-CrxCy-Ni coatings, Wear 442–443 (2020) 203114, https://doi.org/10.1016/j.wear.2019.203114.

[40] K. Torkashvand, S. Joshi, V. Testa, F. Ghisoni, S. Morelli, G. Bolelli, L. Lusvarghi, F. Marra, M. Gupta, Tribological behavior of HVAF-sprayed WC-based coatings with alternative binders, Surf. Coat. Technol. 436 (2022) 128296, https://doi.org/10.1016/j.surfcoat.2022.

[41] X. Chen, X. Wang, D. Fang, A review on C1s XPS-spectra for some kinds of carbon materials, Fullerenes Nanotubes and Carbon Nanostructures 28 (2020) 1048–1058, https://doi.org/10.1080/1536383X.2020.1794851.